Schottky Diode Derating for Survivability in a Heavy Ion Environment

Megan C. Casey, *Member, IEEE*, Jean-Marie Lauenstein, *Member, IEEE*, Raymond L. Ladbury, *Member, IEEE*, Edward P. Wilcox, *Member, IEEE*, Alyson D. Topper, and Kenneth A. LaBel, *Member, IEEE*

***Abstract*—In this paper, we irradiate a number of silicon power Schottky diodes from a variety of manufacturers. The tested diodes represent a wide assortment of reverse voltages and forward currents. Additionally, we review correlations between single-event failures in Schottky diodes and device electrical parameters. The spatial locations of failures in the diode are discussed, as well as a possible explanation for why the failures occur. Based on these correlations to date, we propose a derating scheme for Schottky diodes flown in a heavy ion environment and suggest screening procedures for decreasing the risks of such failures.**

***Index Terms*—Radiation effects, single-event effects, Schottky diodes, single-event burnout, single-event charge collection, diodes, heavy ion testing, heavy ions, defects, radiation effects in devices, radiation hardness assurance, radiation hardness assurance testing, semiconductor device radiation effects, and silicon.**

I. Introduction

UNTIL THE last few years conventional wisdom held that single-event effects (SEEs) could be neglected in silicon diodes, as long as voltages were below several hundred volts [1-10]. This situation changed in the fall of 2011, when two SEE tests of DC-DC converters from two different manufacturers revealed a hitherto unknown destructive SEE mechanism in a Schottky diode [11-15]. When these failures were reproduced in the diode piece parts, the NASA Electronic Parts and Packaging (NEPP) Program undertook the task to elucidate the failure mechanism, ascertain how brown the concern was, and assess the hardness assurance implications and mitigation techniques for the threat.

Initially, the only parts tested were the Schottky diodes internal to the DC-DC converters in which the failures were observed. During this testing, it was quickly determined that the parts are only sensitive when reverse biased, and the diodes become less sensitive to heavy ions with increasing angle of incidence (i.e., normal incidence is the worst case). Further, the sensitivity also appears to decrease with increasing temperature. This is all crucial information for determining failure rates and discerning the failure mechanism, but still does not tell us how these parts may actually be flown in a heavy-ion environment. In this work, we present the results of irradiating a wide range of high-power silicon Schottky diodes and present a derating scheme for use of these parts in radiation environments. Additionally, we discuss correlations between failures and several electrical parameters inherent to the tested parts.

This work was submitted for publication on July 10, 2015. It was supported by the NASA Electronic Parts and Packaging Program.

Megan C. Casey, Jean-Marie Lauenstein, Raymond L. Ladbury, and Kenneth A. LaBel are with NASA/GSFC, Code 561.4, Greenbelt, MD 20771 (USA), emails: megan.c.casey@nasa.gov, jean.m.lauenstein@nasa.gov, raymond.l.ladbury@nasa.gov, kenneth.a.label@nasa.gov.

Edward P. Wilcox and Alyson D. Topper are with ASRC Federal Space and Defense, Inc. (AS&D, Inc.), 7515 Mission Drive, Suite 200, Seabrook, MD 20706, work performed for NASA Goddard Space Flight Center (GSFC), emails: ted.wilcox@nasa.gov and alyson.d.topper@nasa.gov.

II. Test Facilities and Experimental Set-up

A. Parts Tested

A total of 45 types of Schottky diodes from ten different manufacturers were tested in this work. All of the devices under test (DUTs) presented in this work were tested at Lawrence Berkeley National Laboratory's (LBNL) 88" cyclotron using the 10 MeV/amu beam cocktail [16]. Table I shows the beam characteristics for the ion used, Xe.

TABLE I
Heavy Ion Beam Characteristics

Ion	Energy (MeV)	Cocktail (MeV/amu)	LET (MeV-cm^2/mg)	Range in Si (μm)
^{54}Xe	1233	10	58.8	90

All of the parts tested are silicon power Schottky diodes, representing a wide range of commercially available diodes. Table II shows the diodes tested, as well as relevant electrical parameters as specified in the manufacturer datasheets. Before irradiation, the parts were chemically delidded, and mounted on daughtercards. The tested diodes represent a mix of both single and dual parts. The dual parts are either manufactured in a common cathode configuration on the same die or they were packaged as a common cathode with two separate die attached to the same package. The basic schematic for both of these configurations is shown in Fig. 1. When irradiating the dual parts, voltage was only applied to one side at a time, allowing

TABLE II
THE SCHOTTKY DIODES IRRADIATED IN THIS WORK AND SELECT ELECTRICAL PARAMETERS AS SPECIFIED IN THE MANUFACTURERS' DATASHEETS

Manufacturer	Part Number	Single or Dual Part	Reverse Voltage (V)	Forward Current (A)	Max Forward Voltage @I_F (V)	Max Reverse Current (mA)	Number of Parts Tested
Diodes Inc.	MBR2045	Dual	45	10	0.64	0.1	3
Diodes Inc.	MBR2060	Dual	60	10	0.81	0.1	3
Diodes Inc.	MBRF20100	Dual	100	10	0.84	0.05	4
Diodes Inc.	MBRF30100	Dual	100	15	0.84	0.5	4
Diodes Inc.	MBR20200	Dual	200	10	0.89	0.1	4
Fairchild Semiconductor	FYPF1545	Dual	45	7.5	0.55	1.0	3
Fairchild Semiconductor	FYPF2045	Dual	45	10	0.55	1.0	3
Fairchild Semiconductor	FYPF2006	Dual	60	10	0.58	1.0	3
Fairchild Semiconductor	FYPF1010	Dual	100	5	0.75	1.0	3
Fairchild Semiconductor	FYPF2010	Dual	100	10	0.77	0.1	3
Fairchild Semiconductor	MBR3045	Dual	45	15	0.62	1.0	4
Fairchild Semiconductor	MBR20100	Dual	100	10	0.80	0.2	3
Fairchild Semiconductor	MBR20200	Dual	200	10	0.90	0.2	3
International Rectifier	10YQ045C	Single	45	5	0.73	0.5	3
International Rectifier	16SCYQ045C	Single	45	8	0.50	0.4	3
International Rectifier	16SCYQ060C	Single	60	8	0.58	0.68	3
International Rectifier	15CGQ100	Single	100	15	0.95	0.5	3
International Rectifier	16CYQ150C	Single	150	8	0.91	0.5	4
Microsemi	FST30100	Dual	100	15	0.85	0.5	3
NXP Semiconductor	NSXPS20H100	Dual	100	10	0.77	0.0045	3
ON Semiconductor	MBRF2045	Dual	45	10	0.64	0.1	4
ON Semiconductor	MBR4045	Dual	45	20	0.70	1.0	3
ON Semiconductor	MBR6045	Dual	45	30	0.62	1.0	4
ON Semiconductor	MBRB2060	Dual	60	10	0.80	0.15	3
ON Semiconductor	MBR2080	Dual	80	10	0.85	0.1	3
ON Semiconductor	MBRF20100	Dual	100	10	0.85	0.15	3
ON Semiconductor	MBR20200	Dual	200	10	0.90	1.0	33
Power Integrations	LXA03T600	Single	600	3	3.10	0.25	11
Power Integrations	LXA20T600	Single	600	20	3.10	0.25	11
Rohm Semiconductor	RB205T-60	Dual	60	7.5	0.58	0.6	3
STMicroelectronics	STPS1045	Dual	45	10	0.75	0.1	2
STMicroelectronics	STPS4045	Dual	45	20	0.76	0.2	4
STMicroelectronics	STPS40M60	Dual	60	20	0.595	0.11	4
STMicroelectronics	STPS20100	Dual	100	10	0.78	0.03	6
STMicroelectronics	STPS30H100	Dual	100	15	0.80	0.005	3
STMicroelectronics	STPS20200	Dual	200	10	0.86	0.015	4
STMicroelectronics	STPS60SM200	Dual	200	30	0.83	0.05	3
Vishay Semiconductor	MBR4045	Dual	45	20	0.60	1.0	3
Vishay Semiconductor	MBR20100	Dual	100	10	0.80	0.1	3
Vishay Semiconductor	MBR60100	Dual	100	30	0.82	0.1	3
Vishay Semiconductor	MBR20H200	Dual	200	10	0.88	0.005	3
Vishay Semiconductor	SBL8L40	Single	40	8	0.50	1.0	3
Vishay Semiconductor	SBL1040	Single	40	10	0.60	1.0	3
Vishay Semiconductor	SBL3040	Dual	40	15	0.55	1.0	3
Vishay Semiconductor	VS-APH3006	Single	600	30	2.65	0.03	5

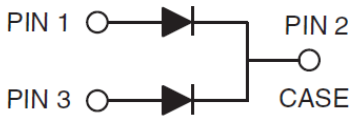


Fig. 1. Common cathode Schottky diode configuration. The anode of each diode can be independently biased, while the cathodes are grounded.

for two datapoints to be obtained from each device. At a minimum, three diodes were tested for each manufacturer part type, and the actual number of diodes of each part type that were tested is also shown in Table II. The tests were conducted using a motherboard capable of mounting six devices under test (DUTs) on daughtercards at a time.

B. Hardness Assurance Technique

While [11-15, 17] showed that Schottky diodes are susceptible to destructive single-event effects, it is not known just how susceptible. NASA Standard "EEE-INST-002: Instructions for EEE Parts Selection, Screening, Qualification, and Derating" [18] requires the drain-source voltage for power MOSFETs be derated to 75% of the device specification. It also specifies that Schottky diodes be derated to 70% of the maximum reverse voltage. These deratings are solely for electrical stress, so the purpose of this work is to determine if that is sufficient for a heavy ion environment, or whether a larger derating is required.

In order to determine what percentage is required to ensure Schottky diodes will survive in a heavy-ion environment, a "go/no go" test was established. All diodes were reverse biased and irradiated with 1233 MeV Xe (LET = 58.8 MeV-

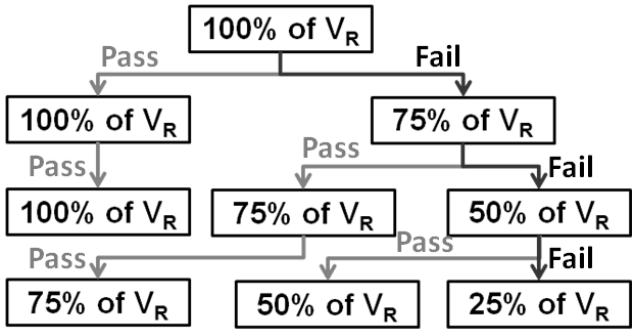


Fig. 2. Test flow for determining how to derate Schottky diodes to ensure survivability in a single-event environment.

cm^2/mg). After each beam run, the forward voltage, reverse voltage, and reverse current were measured.

For each part type, the first diode was irradiated while biased at 100% of the rated reverse voltage. If that part passed, then two more were irradiated at the full reverse voltage to ensure sufficient statistics. However, if the first part failed at 100%, then the second DUT was irradiated while biased at 75% of the reverse voltage. As with the first diode, if the second passed at 75%, then the third (and fourth when available) DUTs were biased at 75% during the test run. If the second DUT failed at 75%, then the third was biased at 50% of the reverse voltage. If the third DUT should fail at 50%, then the fourth (and final) DUT was irradiated at 25% of the rated reverse voltage. This test flow is illustrated in Fig 2.

III. Test Results

Four different conditions were observed during the beam runs. Some parts failed shortly after the beam was turned on. In these cases, the failure always manifested as a short between the anode and cathode, and the source measurement unit (SMU) reached the compliance setting until power was removed. In this work, this is described as a catastrophic failure, and an example is shown in Fig. 3. The second response we observed showed an incremental increase in reverse current during the beam run. For this kind of degradation, individual ions cause discrete damage, corresponding to stepwise increases in reverse current. Each of these increases were larger than the maximum specified reverse current. (See Fig. 4.) Then, while measuring the post-rad parameters, a portion of these parts exhibited decreased reverse voltages, and the reverse current greatly increased, often to the point where the SMUs reached compliance. This

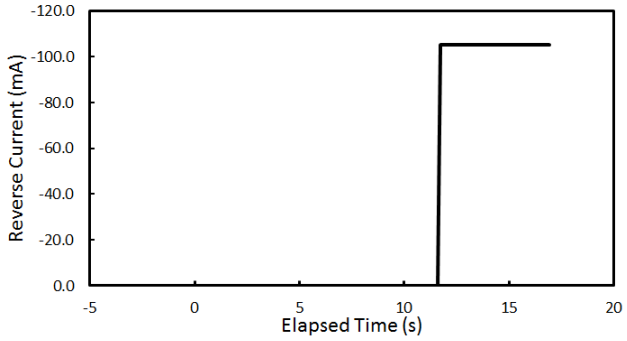


Fig. 3. A catastrophic failure observed while a DUT was being irradiated. The anode and cathode shorted due to the heavy ion strike, and the current was only limited by the SMU. After irradiation, the reverse voltage was well below the specification, as well as below the pre-irradiation measurements. Typically, the forward voltage was also affected in these cases.

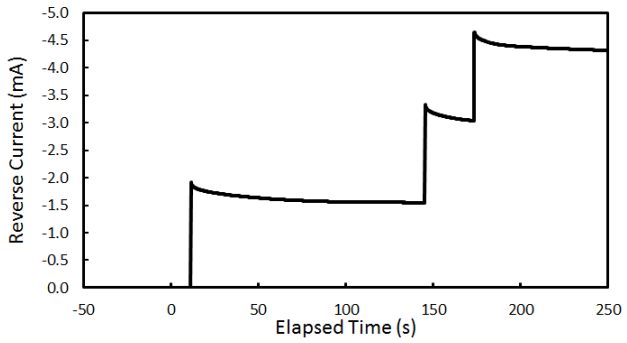


Fig. 4. A type of degradation observed while a DUT was being irradiated. In this case, each increase in reverse current exceeded the manufacturer's specified maximum for reverse leakage current. The electrical parameters measured after irradiation were outside of the manufacturer's specification. This was classified as a device failure.

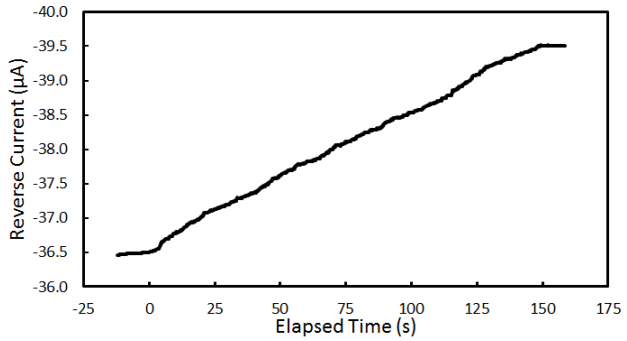


Fig. 5. A type of degradation observed while a DUT was being irradiated. The electrical parameters measured after irradiation remained within the manufacturer's specifications, and these devices were classified as passing.

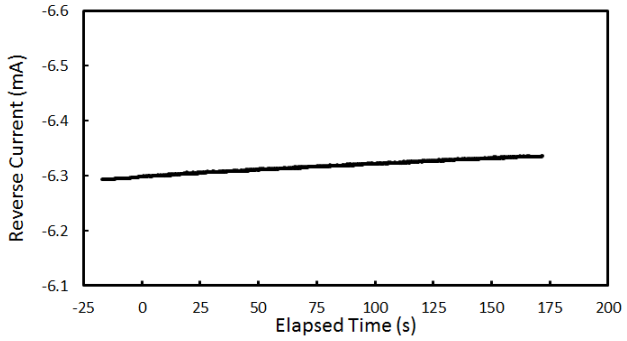


Fig. 6. The reverse current of a part that experienced only minimal charge collection while being irradiated. All tested parameters remained within specification. Parts that experienced this condition were considered to have passed.

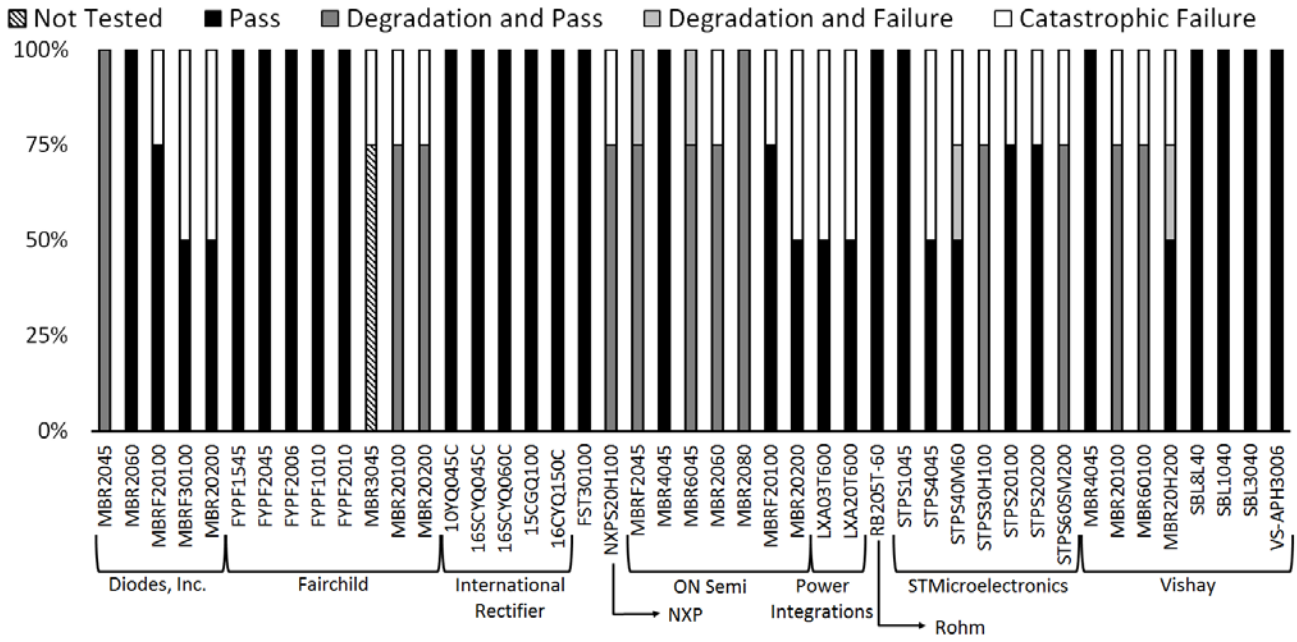


Fig. 7. A summary of the result of irradiating 38 different Schottky diode part types. The white indicates the percent of rated reverse voltage where immediate catastrophic failure occurred. Light gray indicates the percent of rated reverse voltage where degradation was observed during the run, and then the post-irradiation measurements indicated the device had failed. Dark gray indicates degradation was observed, but all post-run parameters were within specification. Black indicates the parts passed with no degradation; while the black and white shaded area indicates the conditions were not tested in that device.

condition was also considered a device failure. The example shown in Fig. 5 shows a part where ions caused slow, continual increases in the reverse current during the beam run that was remained after the beam was turned off. In this case, the electrical parameters measured after irradiation all remained within specification. These parts were considered to have passed. The final condition was simply that charge collection was observed during the beam run, and the post-run measurements were all within specifications. In this case, no degradation or failures were observed. An example is shown in Fig. 6.

In previous work, when a threshold for failure has been found, it has been at several thousand volts. In this previous work. Failures have been observed at a number of ions, and typically all of the failures have been at very high voltages (1050 V [10], 1700 V [6], 2000 V [3], 2500 V [2], 2700 V [9], 3500 V [9], ≥3600 V [1], 4000 V [3, 5, 7], 4500 V [2, 4], 5000 V [4], and >6000 V [4]). However, in [7], the authors observed that failures could occur at breakdown voltages (another name for reverse voltage) as low as 500 V. In this work, failures were observed in Schottky diodes at rated reverse voltages as low as 45 V. While in the previous work, the tested parts were not Schottky diodes, but p-i-n or p-n diodes.

Fig. 7 shows a summary of all the results of this testing for each part type. Of the 45 different parts tested, 20 passed with no degradation or failures during the beam run when biased at 100% of the rated reverse voltage. This is shown with the solid black bars in the figure. Two parts showed degradation when biased at 100%, but all parameters were within specification during the post-run measurements (shown as solid dark gray bars). None of these passing with degradation parts were irradiated at lower voltages, but presumably no degradation would have been observed for such runs. The remaining 23 part types experienced some sort of failure when biased at 100% of the reverse voltage, either catastrophic failure (21 part types) or degradation during the run and failure in the post-run measurements (2 part types).

When the two parts that experience degradation and failure were tested at 75% of their reverse voltages, they both experienced degradation, but all the post-rad measurements, this time, were within specification. These are indicated by the bars with light gray from 75% to 100% and the rest of the bar is dark gray. Of the 21 that saw catastrophic failure, three passed with only charge collection for the 75% derating. In Fig. 7, these are white from 75% to 100% and then black for the rest of the bar. 8 parts also passed at 75%, but they did exhibit degradation while being irradiated. These are indicated with white and dark gray bars. Two parts also showed degradation, but failed due to the parameters being out of specification post-rad. These part types were then further derated to 50%, at which point they both passed with no degradation. These are shown with white from 75% to 100%, light gray from 50% to 75%, and then black from 0% to 50%. Eight parts that experienced catastrophic failure at 100% also experienced catastrophic failure at 75% of their reverse voltage. When derated down to 50%, no failures or degradation were observed. These are indicated by white from 50% to 100%, and then black from 0% to 50%. The only remaining part tested, which is shown as white from 75% to 100% and then shaded with white and black hash lines from 0% to 75%, passed with only minimal charge collection for the

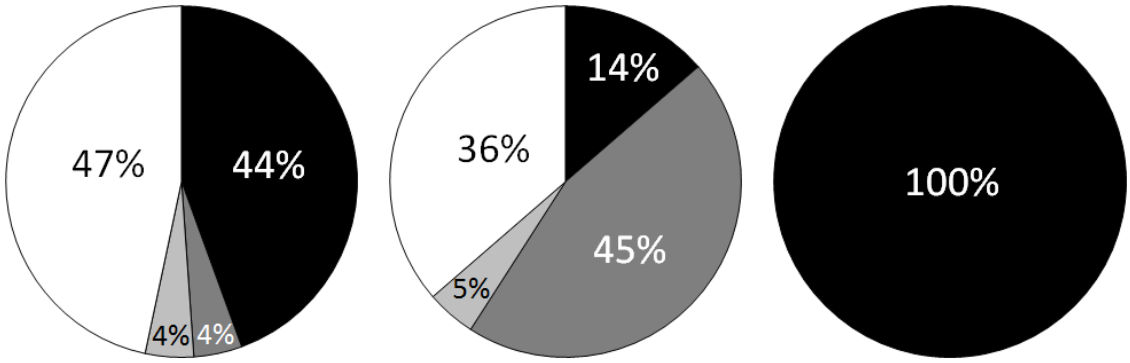


Fig.8. When the reverse voltage is decreased from (a) 100% to (b) 75% to (c) 50% of the rated reverse voltage, the number of devices that fail during irradiation descreases until all parts pass.

first two DUTs tested. However, the other two experienced catastrophic failure. Unfortunately, no more DUTs were available at the time for testing, so it could not be determined at the time whether these parts would have failed at 75% of the rated voltage or less. Figs. 8a-8c graphically summarize the passes and fails for each derating condition described above. In these figures, when a part passes at the higher voltage, it is then not included in the lower derating figures.

As can be seen in these figures, for all parts tested in this work, no DUTs failed or degraded when biased at 50%. While no parts were irradiated at the 70% minimum derating required by EEE-INST-002, the testing completed at 75% derating is near enough when considering part-to-part variability. This electrical stress derating is likely not sufficient for single-event effects, and a more aggressive 50% derating should be used.

Although it appears that a 50% derating on reverse voltage may be sufficient to allow use of Schottky diodes in heavy-ion environments, such a derating may not be possible in all situations. It would also be useful to have methods for screening candidate parts based on their manufacturer specifications so as to select parts that pose minimum risk. No relationship was immediately obvious; the failures ranged across all reverse voltages and forward currents. In the next sections, we discuss whether the barrier heights, reverse currents, and forward voltages might correlate with failure risk.

A. Implication of Barrier Height on Failures

Barrier height in Schottky diodes affects a variety of parameters, including leakage current and forward voltage. Devices with high barrier heights have high forward voltages (due to the forward current dependence on barrier height) and, at elevated temperature, high leakage currents. Likewise, low barrier height diodes have low forward voltage and low leakage current at elevated temperatures. Several manufacturers, including Vishay and Diodes, Inc., have low-barrier-height product lines, which are also advertised as having low forward voltages. Part numbers from these lines generally start with "SBL," three of which was investigated in this work.

The die size also has an implication on the leakage current and forward voltage, but typically the die size is chosen such that the current density remains at reasonable levels. Then, the barrier height is adjusted until the other parameters reach acceptable levels. Barrier height is not a parameter typically listed in datasheets, but can be calculated from device measurements or derived from the part datasheet.

By employing the forward current equation for moderately-doped Schottky diodes [18]

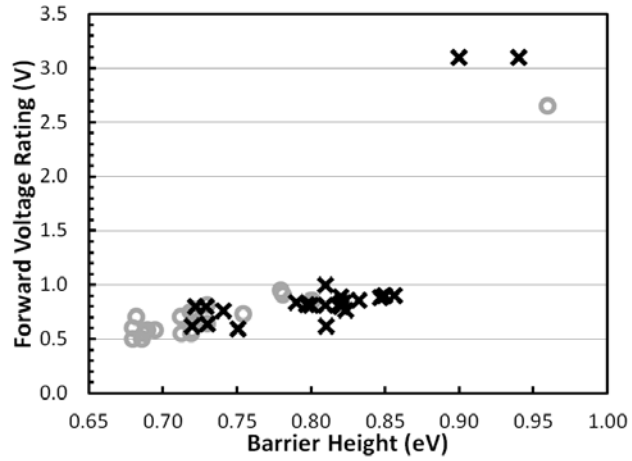
$$J = A^{**}T^2 e^{-\frac{q\varphi_{Bo}}{kT}} e^{\frac{q(\Delta\varphi+V)}{kT}} \quad (1)$$

and deriving the zero-volt current density, we can solve for the barrier height [18]:

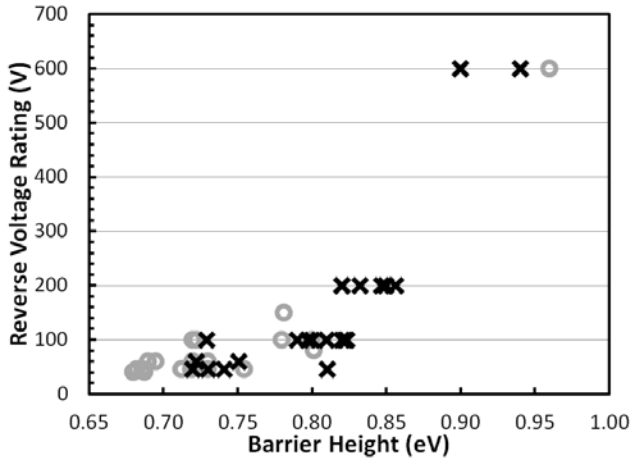
$$\varphi_{Bn} = -\frac{kT}{q}\ln\left(\frac{A^{**}T^2}{J_S}\right) \quad (2)$$

To find the zero-volt current density, J_S, the zero-volt current, I_S, and the active die area are both required. The active die area can be approximated by measuring the die dimensions of the die and multiplying by 90%. The zero-volt current can be derived by measuring the forward currents at a minimum of three forward voltages, and then extrapolating to the current at 0 V. The voltages at which the forward currents are measured must be sufficiently low to ensure the currents are in the flat region of the curve on a log scale. However, designers often will not have parts on-hand for making these measurements, especially when the decision has not been made as to which parts will be chosen. In this case, the required datapoints can be approximated from the datasheet. I_F-V_F curves are typically included in each datasheet for a number of temperatures, and the necessary I_F values can be obtained from these curves. Again, the values on the graph chosen must be within the flat region of the I_F-V_F curve. I_S would be then be extrapolated in the same way as when the I_F values are measured.

The temperatures in equations (1) and (2) are in Kelvin, and, in our case, are room temperature, approximately 300K. All of the remaining terms in the equations are constants. k is Boltzmann's constant and is defined as $8.617332\text{x}10^{-5}\ \frac{eV}{K}$. q, in this case, is charge in eV, which is simply 1.0. Finally, the A** used here is the theoretical Richardson's constant,

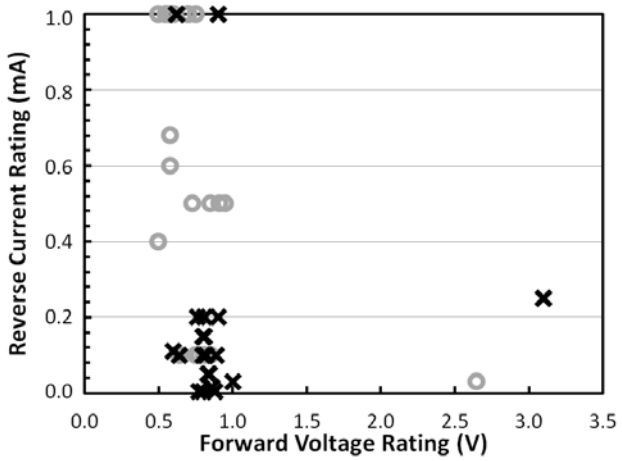


(a)

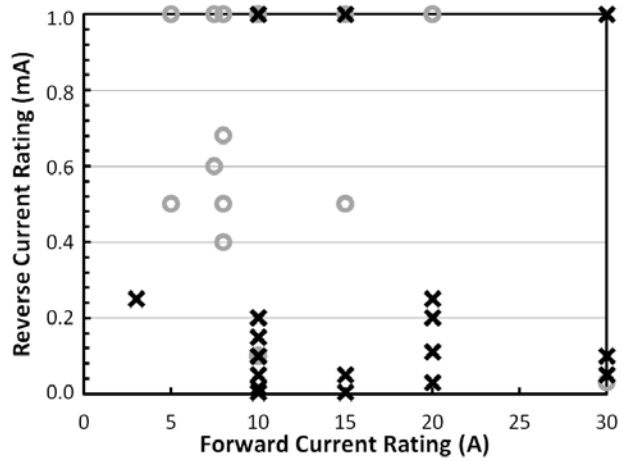


(b)

Fig. 9. Failures observed at 100% of the rated reverse voltage in the tested Schottky diodes show a strong correlation with the parts' barrier heights. The (a) forward voltage and (b) reverse voltage are shown versus the barrier height for all the parts tested.



(a)



(b)

Fig. 10. Failures observed at 100% of the rated reverse voltage in the tested Schottky diodes show a strong correlation with the manufacturers' rated reverse current for each part. The reverse current verse the (a) forward voltage and versus (b) forward current are shown versus the barrier for all the parts tested.

$1.20173 \times 10^6 \frac{A}{m^2 K^2}$. The material and orientation of the lattice structure can affect this value, but the theoretical value is fine for our approximations here.

Figs. 9a and 9b show the failures (black Xs) and passes (gray Os) as a function the barrier height, as well as the forward voltage and the reverse voltage, respectively. There is a clear line at barrier heights of approximately 0.72 eV. Below this point, no failures were observed in parts biased at 100% of the reverse voltage. Parts with barrier heights greater than 0.72 eV almost exclusively failed during the beam runs while biased at 100% of the reverse voltage. Parts with barrier heights near or above 0.72 eV should be tested if heavy ion data does not exist.

B. Implication of Reverse Current on Failures

Much as with barrier height, there is a strong dependence of the failures on the reverse current rating. Figs. 10a and 10b show the fails and passes when biased at 100% of the rated reverse voltage as a function of reverse current versus forward voltage and reverse voltage, respectively. The parts in which failure was observed are tightly grouped together for parts with a rated reverse current less than 200 μA. There are, however, three failures well above of this grouping (two are overlapping in Fig. 10a.)

If the same figures are plotted for the data acquired when the parts are biased at 75% of the rated reverse voltage, as in Figs 11a and 11b, all but one of the anomalous failures from the previous dataset becomes a pass. Interestingly, the remaining failure that is outside the low reverse current grouping was the ON Semiconductor MBR20200CT. This was the first part in which these failures were observed in a DC-DC converter. This part has also been fully characterized over a wide range of voltages [15], and has been found to be susceptible to ions as light as Ne, which has an LET of 3.5 MeV-cm^2/mg. It is possible this part is just particularly susceptible to heavy ions, moreso than any other part we have tested.

C. Implication of Forward Voltage on Failures

Because forward voltage depends on the barrier height, and it has already been shown that there is a strong correlation between barrier height and failures, it is necessary also to

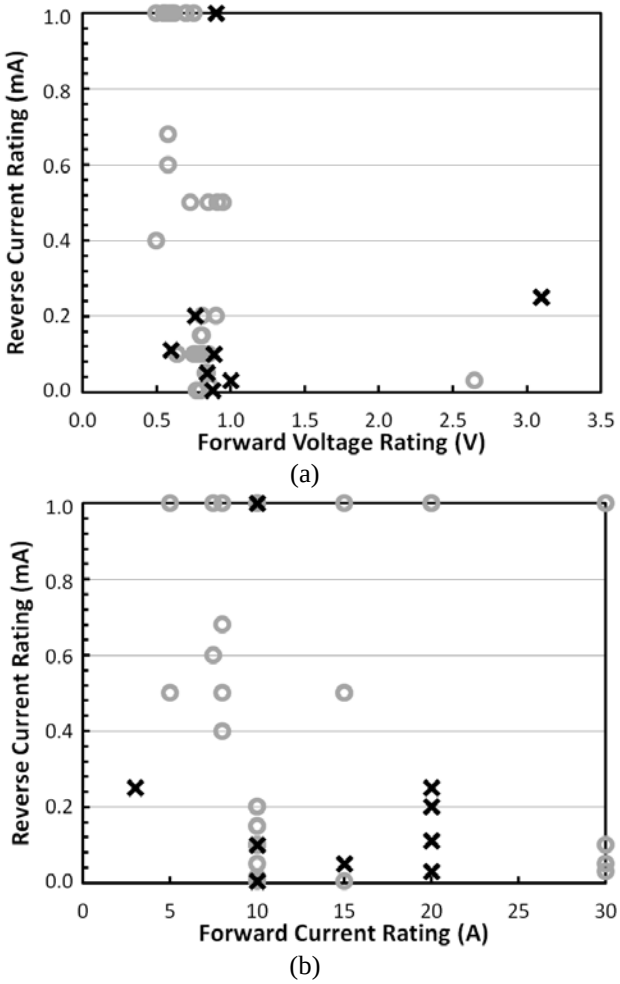


Fig. 11. When the derating is reduced to 75% of the reverse voltage, the failures in Schottky diodes show a stronger relationship with the manufacturers' rated reverse current for each part. The reverse current verse the (a) forward voltage and versus (b) forward current are shown versus the barrier for all the parts tested.

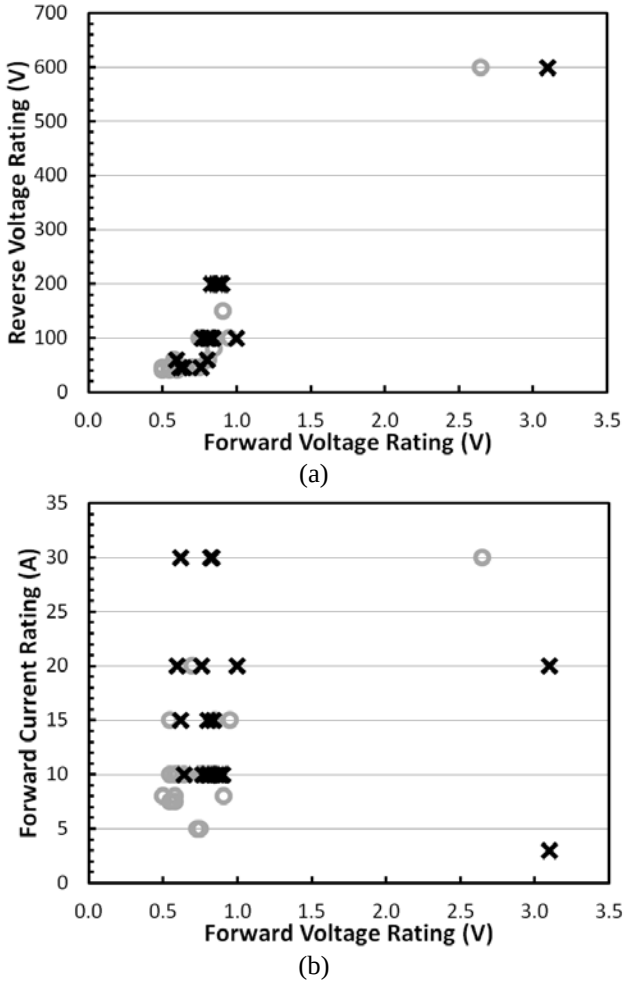


Fig. 12. There appears to be a weaker dependence on the forward voltage with device failures. Shown here are the (a) reverse voltage and (b) forward currents.

compare the forward voltage of these parts and the failures. A correlation between the failures and V_F would be especially helpful, since these values are readily found in the datasheets, and no additional derivations or calculations would be required. Figs. 12a and 12b show the failures at 100% of the reverse voltage plotted against the forward voltage. Manufacturers' datasheets typically list several forward voltages, one each for a number of forward current values. The datasheets usually specify the V_F at the per-diode rated reverse current, as well as the per-device (twice the per-diode since these are dual parts.) The forward voltages plotted here are all per-diode. As can be seen in these figures, there is less of a correlation than observed with barrier height. This may be due to the fact that forward voltage is specified at the per-diode forward current, so the specified forward current becomes conflated with the forward voltage. There is no obvious way to normalize the forward voltage across all the part types with different reverse voltages and different forward currents. However, the diodes do appear to be slightly more likely to fail when the forward voltage is greater than or equal to 0.6 V.

IV. Failure Analysis

Optical examination of failures in the DC-DC converters in which these failures were originally observed indicated the locations of the failures were along the guardring and several hundred microns away from the guardring. In other recent Schottky diode destructive SEE analysis, the Aerospace Corporation found that the failure locations were only along the guardring [17].

No failure locations could be observed with the bare eye in the parts irradiated in this work. This is attributable to the current limiting that occurs when the SMUs reach compliance after a failure is observed. Because the failed devices are not allowed infinite current, no large failure locations are visible. In order to truly determine the failure location, a thermal camera attached to a microscope was used. A small voltage was applied to the diode until the failure location became heated from the large current flowing from the shorted anode to the cathode. Fig. 12 shows the failure locations found using the thermal camera in (a) Vishay MBR20100CT, (b) ON Semiconductor MBR20200CT, (c) ON Semiconductor MBRF200100CTG, and (d) Fairchild MBR20200CTTU

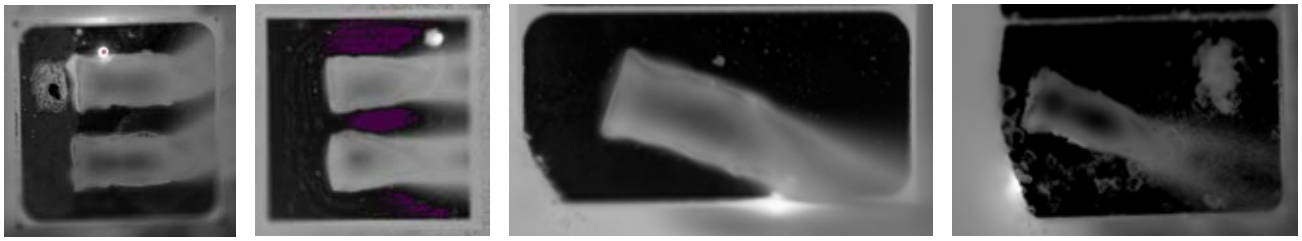


Fig. 13. Thermal images of failure locations in the (a) Vishay MBR20100CT, (b) ON Semiconductor MBR20200CT, (c) ON Semiconductor MBRF200100CTG, and (d) Fairchild MBR20200CTTU.

samples. In the Vishay MBR20100CT and the ON Semiconductor MBR20200CT samples, the failure locations are hundreds of microns away from the guardring. However, in the Vishay part, there is an elevated temperature location in the guardring. All parts are irradiated at normal incidence, so there is no direct path between the initial failure location and the elevated temperature spot on the guardring. Unfortunately, the locations of the ON Semiconductor MBRF20100CTG and the Fairchild Semiconductor MBR202002CTTU are ambiguous. The MBRF20100CTG failure location in this sample may be along the guardring. The Fairchild MBR20200CTTU failure looks like it is under some remaining encapsulant that was not completely etched away. The Xe ion could have been slowed passing through the encapsulant, losing energy, and increasing the ion's LET.

In [21-22], the author observed degradation in n-channel JFET diodes due to single ion strikes. They found the increase in leakage current was due to radiation-induced defects in the depletion region. While the reverse voltages they investigated are much lower (12 V) than the voltages in this work, the degradation signatures are very similar. Additionally, because the failures observed in this work are not solely located along the guardring, it may further indicate that the degradation is caused by junction defects. Further work to explore this explanation is necessary.

V. Conclusions

While the mechanism of the failures is still unknown, at this point, derating to 50% of the reverse voltage appears to ensure Schottky diodes will survive a single-event environment. Several electrical parameters have been identified that show a strong correlation with these failures. These parameters can be used to identify Schottky diodes that are less susceptible to destructive single-event effects. In particular, parts with barrier heights less than 0.72 eV or reverse current specifications greater than 200 μA are recommended. Parts with barrier heights less than 0.72 eV or reverse currents less than or equal to 200 μA should be tested under the specific application conditions. This is especially true if an application requires a part be derating at a percentage greater than 50%.

Additionally, the failure locations from this work are not located solely along the guardring, suggesting that they are not the cause of the failures like previously assumed. Additionally, the location of the failures seems to correspond with previous work on junction defects in JFET diodes.

VI. Acknowledgment

The authors thank NEPP and the Defense Threat Reduction Agency (DTRA) for funding this effort, as well as the members of the Radiation Effects and Analysis Group (REAG) who contributed to the test results presented here: Dakai Chen, Hak Kim, Anthony Phan, Donald Hawkins, Michael Campola, and Stephen Cox. Additionally, the authors would like to acknowledge the personnel at LBNL for their support during beam runs.

References

[1] H. Kabza, H. J. Schulze, Y. Gerstenmaier, P. Voss, J. Wilhelmi, W. Schmid, F. Pfirsch, and K. Platzoder, "Cosmic radiation as a cause for power device failure and possible countermeasures," *Proc. 6th Int. Symp. Power Semiconductor Devices ICs*, Davos, Switzerland, May 1994, pp. 9–12.

[2] H. R. Zeller, "Cosmic ray induced breakdown in high voltages semiconductor devices, microscopic model and phenomenological lifetime prediction," *Proc. 6th Int. Symp. on Power Semiconductor Devices and ICs*, Davos, Switzerland, May 1994, pp. 339–340.

[3] G. Soelkner, P. Voss, W. Kaindl, G. Wachutka, K. H. Maier, and H.-W. Becker, "Charge carrier avalanche multiplication in high-voltage diodes triggered by ionizing radiation," *IEEE Trans. Nucl. Sci*., vol. 47, no. 6, pp. 2365–2372, Dec. 2000.

[4] P. Voss, K. Maier, H. Becker, E. Normand, J. Wert, K. Oberg, and P. Majewske, "Irradiation experiments with high voltage power devices as a possible means to predict failure rates due to cosmic rays," *Proc. 9th Intl. Symp. Power Semiconductor Devices ICs*, Weimar, Germany, May 1997, pp. 169–173.

[5] K. H. Maier, A. Denker, P. Voss, and H.-W. Becker, "Single-event burnout in high power diodes," *Nucl. Instrum. Methods Phys. Res. B*, vol. 146, pp. 596–600, Dec. 1998.

[6] G. Busatto, F. Iannuzzo, F. Velardi, and J. Wyss, "Non-destructive tester for single event burnout of power diodes," *Microelectron. Reliab.*, vol. 41, pp. 1725–1729, Sept. 2001.

[7] G. Soelkner, W. Kaindl, H.-J. Schulze, and G. Wachutka, "Reliability of power electronic devices against cosmic radiation-induced failure," *Microelectron. Reliab*., vol. 44, pp. 1399–1406, Sept. 2004.

[8] A. M. Al-badri, D. G. Walker, T. S. Fisher, and R. D. Schrimpf, "Simulation of single event failure in power diodes," *Proc. Int. Mechanical Engineering Congress Expositions*, New Orleans, LA, Nov. 2002, pp. 17–22.

[9] A. M. Albadri, R. D. Schrimpf, D. G. Walker, and S. V. Mahajan, "Coupled Electro-Thermal Simulations of Single Event Burnout in Power Diodes," *IEEE Trans. on Nucl. Sci.*, vol.52, no.6, pp.2194-2199, Dec. 2005.

[10] T. Shoji, S. Nishida, K. Hamada, and H. Tadano, "Observation and Analysis of Neutron-Induced Single-Event Burnout in Silicon Power Diodes," *IEEE Trans. on Power Electronics*, vol.30, no.5, pp.2474-2480, May 2015.

[11] M. V. O'Bryan, K. A. LaBel, J. A. Pellish, J.-M. Lauenstein, D. Chen, C. J. Marshall, M. C. Casey, R. A. Gigliuto, A. B. Sanders, T. R. Oldham, H. S. Kim, A. M. Phan, M. D. Berg, P. W. Marshall, R. L. Ladbury, E. P. Wilcox, A. J. Boutte, P. L. Musil, and G. A. Overend, "Compendium of Single Event Effects for Candidate Spacecraft Electronics for NASA," *2012 IEEE Radiation Effects Data Workshop (REDW)*, pp.1-9, 16-20 July 2012.

[12] Observed Diode Failures in DC-DC Converters, available online: http://nepp.nasa.gov/workshops/etw2012/talks/Tuesday/T15_Gigliuto_Observed_Diode_Failures.pdf

[13] Destructive Single-Event Failures in Schottky Diodes, available online: https://nepp.nasa.gov/workshops/etw2013/talks/Wed_June12_2013/1430_Casey_Schottky_Diode_Radiation_Failures.pdf

[14] M. V. O'Bryan, D. Chen, M. J. Campola, M. C. Casey, A. D. Topper, K. A. LaBel, J. A. Pellish, J-M Lauenstein, R. A. Gigliuto, E. P. Wilcox, R. L. Ladbury, M. D. Berg, and R. R. Davies, "Compedium of Recent Single Event Effects for Candidate Spacecraft Electronics for NASA," *Radiation Effects Data Workshop (REDW), 2013 IEEE*, pp.1-8, 8-12 July 2013.

[15] Destructive Single-Event Failures in Schottky Diodes, presented at the 2013 Nuclear and Space Radiation Effects Conference, available online: https://nepp.nasa.gov/files/24642/2013_n246_NSREC_Casey_I-1_Diode_pres.pdf.

[16] Lawrence Berkeley National Laboratory, Berkeley Accelerator Space Effects Facility, 88-Inch Cyclotron Cocktails and Ions, available online: http://cyclotron.lbl.gov/base-rad-effects/heavy-ions/cocktails-and-ions

[17] J. George, R. Koga, R. M. Moision, and A. Arroyo, "Single Event Burnout Observed in Schottky Diodes", *Radiation Effects Data Workshop (REDW), 2013 IEEE*, pp.1-8, 8-12 July 2013.

[18] EEE-INST-002: Instructions for EEE Parts Selection, Screening, Qualification, and Derating, available online: https://nepp.nasa.gov/docuploads/FFB52B88-36AE-4378-A05B2C084B5EE2CC/EEE-INST-002_add1.pdf

[19] S. M. Sze, "Metal-Semiconductor Contacts," in *Physics of Semiconductor Devices (Second Edition)*, John Wiley & Sons, New York (1981), pp. 279-297.

[20] Application Note: Design Guildelines for Schottky Rectifiers, Vishay General Semiconductor, available online: http://www.vishay.com/docs/88840/andesign.pdf

[21] E. C. Auden, "Heavy Ion-Induced Single Particle Displacement Damage in Silicon," Ph.D. dissertation, Dept. of Elect. Eng. and Comp. Sci., Vanderbilt University, Nashville, TN, 2013.

[22] E. C. Auden, R. A. Weller, M. H. Mendenhall, R. A. Reed, R. D. Schrimpf, N. C. Hooten, and M. P. King, "Single particle displacement damage in silicon," *IEEE Trans. Nucl. Sci.*, vol. 59, pp. 3054 – 3061, Dec 2012.